

INCLUSIVE PRODUCTION OF NEUTRAL STRANGE PARTICLES IN ANTIDEUTERON-NUCLEI INTERACTIONS AT 12.2 GeV/c

B.V.Batyunya, I.V.Boguslavsky, D.Bruncko¹,
C.Coca², I.M.Gramenitsky, K.S.Medved,
T.Ponta², I.B.Šimkovicova

The data on inclusive production of Λ and K_S^0 in antideuteron-deuteron, antideuteron-carbon and antideuteron-lead interactions at 12.2 GeV/c are reported. The results are given on relative yields, rapidity distributions, average multiplicities of associated charged particles, and kinematical characteristics of neutral strange particles. The possible difference of production mechanisms for K_S^0 - and Λ -particles, as well as the enhancement of Λ -hyperons yield in events with the developed cascade, are also discussed. The data were obtained while irradiating the 2 m bubble chamber LUDMILA with a separated antideuteron beam at the Serpukhov accelerator.

The investigation has been performed at the Particle Physics Laboratory, JINR.

Инклюзивное образование
нейтральных странных частиц
в антидейтрон-ядерных взаимодействиях
при импульсе 12,2 ГэВ/с

Б.В.Батюня и др.

В работе представлены экспериментальные данные по инклюзивному образованию Λ - и K_S^0 -частиц во взаимодействиях антидейтронов с ядрами дейтерия, углерода и свинца при 12,2 ГэВ/с. Приведены результаты по относительным выходам, быстротным распределениям, средним ассоциативным множественностям заряженных частиц в первичном взаимодействии и кинематическим характеристикам нейтральных странных частиц. Обсуждаются также возможное различие механизмов образования K_S^0 - и Λ -частиц и увеличение выхода Λ -гиперонов в событиях с развитым каскадом. Данные были получены при облучении 2-метровой пузырьковой камеры ЛЮДМИЛА сепарированным пучком антидейтронов на ускорителе ИФВЭ.

Работа выполнена в Лаборатории сверхвысоких энергий ОИЯИ.

¹Institute of Experimental Physics, Slovak Acad. of Sciences, Kosice, Slovakia

²Central Institute of Physics, Bucharest, Romania

1. Introduction

Till the present moment, the processes of $\bar{N}N$ annihilation have been studied thoroughly. At the same time, the mechanisms of antinucleon-nucleus interactions are still relatively unknown. The nucleus, especially a heavy one, can influence the elementary $\bar{N}N$ interaction, and modify seriously the final hadron state formation picture.

The creation of pure and intensive antiproton beams has given new possibilities of studying some unusual phenomena occurring at antiproton annihilation in nuclear matter [1,2]. Annihilation could release rather large energy (~ 2 GeV) in a small volume (~ 1 fm³) of nuclear medium [25], that could lead to the creation of «hot drops» inside the nucleus. Also, the production of several pions in a small region and conversion of a large fraction of annihilation energy into the kinetic energy of the nucleons could result in some specific effects like «nuclear explosion» [3].

It is expected that if high energy density could be reached in some region inside the nucleus, these extreme conditions would lead to the formation of deconfined phase of nuclear matter. The first predicted signature of the deconfined phase formation was an enhancement of s and \bar{s} quarks concentration in a quark-gluon plasma, relative to $u\bar{u}$ and $d\bar{d}$ pairs [4], and the strange particle production was intensively studied in this context [5].

Yet there is no unambiguous experimental evidence of the existence of quark-gluon plasma. But the processes of strange particle production in hadron-nucleus collisions themselves are of great interest, as the strange particles are very sensitive to any details of the production mechanism. Strange quarks are not «prepared» in the projectile antinucleon and they should be produced from the sea quarks on early stage of the interaction, whereas non-strange quark pairs be produced at all stages.

The number of experimental data on strangeness enhancement in antinucleon-nucleus interactions is limited. The statistics in bubble chamber experiments is usually low, whereas the rejected acceptance gives rise to various methodical difficulties in counter experiments. Concerning the data on neutral strange particle production, there were only a few published results [6—15].

In all these experiments, at energies of 0—4 GeV, the unexpectedly high Λ -hyperon production was observed. Even at LEAR energies, the Λ yields below threshold are large and comparable to K_s^0 yields, that could not be explained by interaction with a single nucleon. One can find the review of the experimental situation in [2].

Various models have been used to explain the high Λ yield. In [17] the strangeness enhancement in \bar{p} -Ta data at 4 GeV/c were considered to be the result of the supercooled quark-gluon plasma formation at $T < 60$ MeV.

In [18,19] this phenomenon is explained in terms of multinucleon absorption reactions. In the framework of the statistical picture it was found that in $B \geq 1$ annihilation the strangeness production is substantially increased as compared to $B = 0$ annihilation. (B is the baryon number of the annihilating system). But the experimental results on formation frequency of the $B \geq 1$ fireball, are still rather contradictory.

At the same time, the data on Λ and K_s^0 production in \bar{p} -interactions with heavy targets were explained satisfactorily within the framework of the intranuclear cascade models [20—24]. In these models, the strong rescattering effects in antiproton annihilation on nuclei were taken into account. The Λ production characteristics were reproduced under the assumption that strangeness is produced in conventional $\bar{N}N$ processes and then redistributed through subsequent pion-nucleon rescattering and absorption:

$$\bar{N}N \rightarrow \bar{K}K + (m\pi), \text{ followed by} \\ \bar{K}N \rightarrow \Lambda X, \bar{K}NN \rightarrow \Lambda NX;$$

$$\bar{N}N \rightarrow (m\pi) + X, \text{ followed by} \\ \pi^0 p \rightarrow \Lambda K^+, \pi^- p \rightarrow \Lambda K^0;$$

$$\bar{N}N \rightarrow \eta(\omega) + X, \text{ followed by} \\ \eta(\omega) + p \rightarrow \Lambda + K^+, \eta(\omega) + n \rightarrow \Sigma^0 + K^+, \dots$$

The detailed studies of hA interactions at 200 GeV/c by NA5 Collaboration [16] inspired the description of strangeness enhancement in the framework of Dual Parton Model [34]. The role of reabsorption effects for strangeness production at this energy was also discussed [28].

The further studies of strangeness production at various energies, and targets, are of great interest. The characteristics of these processes — particles temperatures, relative yields, rapidity distributions, and especially those characteristics triggered by high charged multiplicities, may reveal possible existence of collective effects in nuclear matter.

2. Antideuteron as a Projectile

At energies lower than 1 GeV, the annihilation cross section is large, so, most of the slow antinucleons interact at the surface of the target nucleus.

Only a small fraction of antinucleon could penetrate deep enough and thermalize the nucleus [3].

At high energies, the ability of annihilation products to interact inside the nucleus is greatly suppressed due to the relativistic growth of the formation length [28,34].

Obviously, there should be an optimum antinucleon energy for excitation of a nucleus. In [25] it was shown that at 6 GeV/c an antinucleon (or antideuteron at 12 GeV/c) is a very good tool to investigate these effects because at this energy antinucleons can penetrate deep enough into a nucleus, and the emitted pions are concentrated in a narrow cone (with the average angle about 10 degrees). Also, the ability of antideuterons to produce the high temperatures in a nucleus due to simultaneous annihilation of both the antinucleons was predicted.

On the contrary, recent cascade calculations [26] have shown that due to the limited dimensions of the excited region both in space and time, the antideuteron does not appear to be a suitable tool to study quark-gluon plasma effects.

The question whether the interactions of antideuterons in nuclei could deliver some information on a short range correlation in the target nuclei was discussed in [35]. It has been found that antideuterons are not an effective tool for these studies, because antibaryons are (on the average) too far from each other.

In this paper we report our experimental data on neutral strange particle production in antideuteron interactions with deuterium, carbon and lead nuclei. We were looking for the peculiarities of neutral strange particle production in $\bar{d}A$ -interactions, that may reflect some interesting dynamics, similar to those found in $\bar{p}A$ -interactions at lower energies.

Antideuteron as a projectile is a more complicated object for analysis than antiproton. At our energy the $\bar{N}N$ annihilations cross section is about 40% of the total inelastic cross section, and there is a large probability for antideuteron to have no annihilation interactions in nucleus at all.

Also, the average radius of an antideuteron is about 1.5 fm compared to the radius of light nucleus and not much smaller than the radius of a heavy nucleus (8 fm for lead). Therefore, if one of antinucleons interacts close to the nucleus edge, another antinucleon with a marked probability passes through or by the nucleus without interaction.

This process allows one to mark the peripheral interactions of antinucleons with the nucleus. The interactions with the registered fast antiproton-spectator are enriched by peripheral $\bar{N}A$ interactions. We expect that the strangeness production should be somewhat different for these events compared with the central collisions.

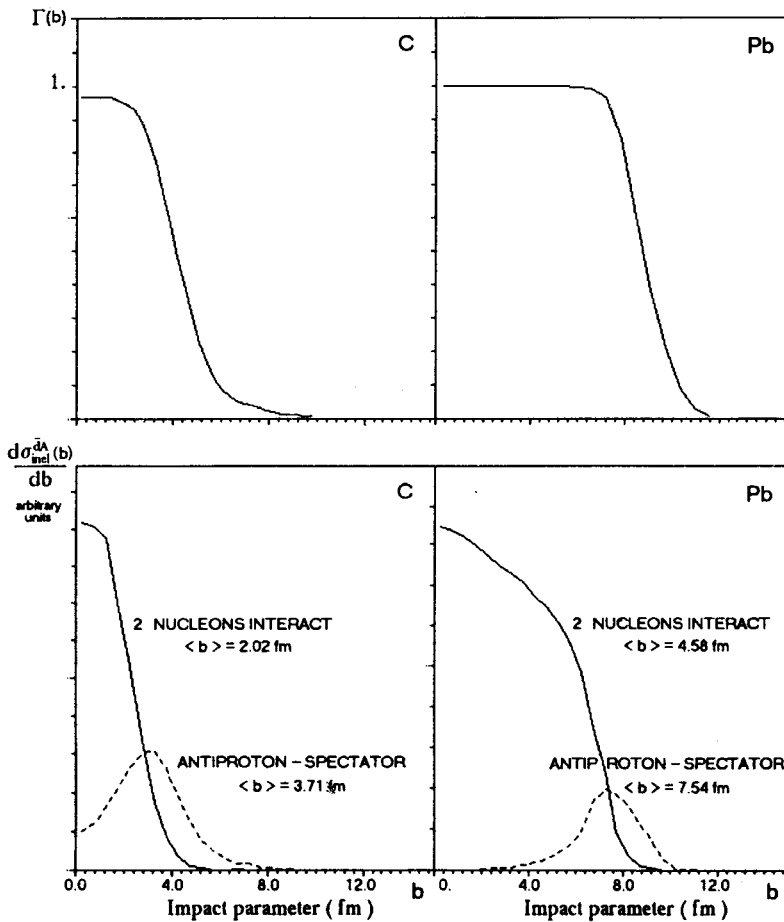


Fig.1. The profile functions for carbon and lead nuclei and antideuteron impact parameter distributions. Dashed lines show the distributions in the case when antiproton does not interact with the nucleus and reveals as a spectator

Fig.1 shows the profile functions for carbon and lead nuclei, and the results of Glauber calculations for $\bar{d}A$ -interactions [27]. The impact parameter distribution shows that in events with antiproton-spectator the second antinucleon interacts close to the surface of the target nucleus.

The number of interactions with fast \bar{p} -spectator decreases while the target nucleus mass grows. In our experiment the registered number of these events was 39%, 23%, and 11% for deuterium, carbon and lead, respectively.

Both — the arrangement of our experiment and data handling procedures were described in detail in [15].

The 2 m HBC LUDMILA was exposed to a 12.2 GeV/c antideuteron beam at the Serpukhov accelerator. Before separation, the ratio of π^- to \bar{d} was as high as $10^6:1$. A two-stage scheme of separation was used to suppress the hadron background. The intensity of antideuterons was about $0.5\bar{d}$ per picture.

Filled with liquid deuterium, the internal track-sensitive target was installed inside the chamber. The main task of the experiment was to study the multinucleon effects in the antideuteron-deuteron interactions. Also, we were able to observe and measure the interactions of beam antideuterons in lexan ($H_{14}C_{16}O_3$) and lead plates inside the chamber. The lexan plate was 12 mm thick and lead plate — 3 mm.

Lexan is not a pure nuclear target. The probability for an antideuteron to interact with various nuclei in lexan was calculated as $P(C/O/H) = 0.74/0.17/0.09$. In this paper, \bar{d} -lexan interactions are denoted as $\bar{d}-C$:

The neutral strange particles were observed through the charged decay modes; four kinematical hypotheses were tried for each V^0 :

$$K_s^0 \rightarrow \pi^+ + \pi^-$$

$$\Lambda \rightarrow p + \pi^-$$

$$\Lambda \rightarrow \bar{p} + \pi^+$$

$$\gamma \rightarrow e^+ + e^-.$$

No attempts have been made to separate Λ ($\bar{\Lambda}$) from Σ^0 ($\bar{\Sigma}^0$) production. The classification of V^0 was based on kinematical fit results as well as ionization data [15].

The total number of registered $\bar{d}A$ interactions and the numbers of measured and corrected vees are presented in Table I.

For the events with antiproton-spectator, the limited number of neutral strange particles did not allow us to perform detailed studies. In this paper, only relative yields are reported for these reactions.

The charged tracks of primary interactions with vees (V^0 or γ) were also measured. The bubble density of the tracks was compared with geometrical program data. We were able to distinguish electrons, pions and protons in the momentum range $P < 1.5$ GeV/c and for *dip* angles less than 65 degrees.

Table 1. Total number of interactions and number of measured and corrected vees in $\bar{d}A$ experiment

REACTION	Fitted, unweighed	Weighed, corrected
$(\bar{d} + \pi^-) + d \rightarrow \text{inelastic}$	7800 scanned	
$(\bar{d} + \pi^-) + d \rightarrow K_s^0 + X$	106	240
$(\bar{d} + \pi^-) + d \rightarrow \Lambda + X$	86	174
$(\bar{d} + \pi^-) + d \rightarrow \bar{\Lambda} + X$	38	72
$(\bar{d} + \pi^-) + d \rightarrow \gamma + X$	229	
$(\bar{d} + \pi^-) + C' \rightarrow \text{inelastic}$	3750 scanned	
$(\bar{d} + \pi^-) + C' \rightarrow K_s^0 + X$	77	167
$(\bar{d} + \pi^-) + C' \rightarrow \Lambda + X$	59	138
$(\bar{d} + \pi^-) + C' \rightarrow \bar{\Lambda} + X$	9	23
$(\bar{d} + \pi^-) + C' \rightarrow \gamma + X$	308	
$(\bar{d} + \pi^-) + \text{Pb} \rightarrow \text{inelastic}$	3890 scanned	
$(\bar{d} + \pi^-) + \text{Pb} \rightarrow K_s^0 + X$	204	479
$(\bar{d} + \pi^-) + \text{Pb} \rightarrow \Lambda + X$	299	597
$(\bar{d} + \pi^-) + \text{Pb} \rightarrow \bar{\Lambda} + X$	7	13
$(\bar{d} + \pi^-) + \text{Pb} \rightarrow \gamma + X$	656	

Beam contamination with negative π^- mesons was an obvious source of systematic errors in our experiment. The contribution from the background interactions was accounted using both: data extrapolating on strange particle production in π^- -nuclei interactions at close energies, and the Monte-Carlo simulated π^- -nuclei events at 12.2 GeV/c, obtained with FRITIOF code. The contribution of V^0 from the background events was the reason of the bigger uncertainties in our final results we had expected.

The beam contamination was estimated at the level of $1.73 \pi^-$ per $1 \bar{d}$. It means that the number of background interactions could reach 35% of all interactions in deuterium target, 45% for lexan and 50% for lead plates. Though this admixture was lower for the events with V^0 , nevertheless the background extraction procedure was the most complicated part of data analysis and the source of permanent troubles.

3. Yield Ratios Λ/K_s^0

In $\bar{p}p$ - and $\bar{p}d$ -interactions at momentum range of 0—12.0 GeV/c, the production cross sections for K_s^0 exceed considerably the corresponding ones for Λ . The typical values for the ratios of production cross sections in elementary \overline{NN} collisions are $R_{\Lambda/K_s^0} = 0.2—0.5$ [11].

Recently, the neutral strange particle production on nuclear targets has been also studied, though not many experimental results have been published:

- the measurements of $\bar{p} + C, Ti, Ta, Pb$ at (0—450) MeV/c [6];
- the KEK measurements of \bar{p} Ta interactions at 4 GeV/c [7];
- the streamer chamber measurement of PS 179 experiment at LEAR ($\bar{p} + He^3, He^4$ and Ne^{20} at rest and at 600 MeV/c) [8—11];
- results on strange particle production obtained at ITEP ($\bar{p} - Xe$ at 0—0.9 GeV/c) [12,13];
- the measurements of ASTERIX ($\bar{p} + N^{14}$ at rest) [14].

The most striking feature of all the data obtained in those experiments, is the unexpectedly high Λ -hyperon production yields. The ratios R_{Λ/K_s^0} were found to be greater for about one order of magnitude than in \overline{NN} interactions [2,11]. Even for stopping antiprotons, the Λ yield turns out to be high and comparable with the K_s^0 production cross section.

Obviously, the strangeness in $\bar{p}A$ reactions is enhanced due to the effect of nuclear medium, and cannot be calculated from \overline{NN} data using simple geometrical extension. At LEAR energies the production of a Λ on a single nucleon is forbidden (as the threshold for reaction $\bar{p}p \rightarrow \Lambda \bar{\Lambda}$ is $p = 1435$ MeV/c), and several nucleons should be obligatory involved into this interaction.

In our experiment, we calculated the ratios:

$$R_{K_s^0} = \frac{N(K_s^0)}{N_{inelastic}}$$

$$R_{\Lambda} = \frac{N(\Lambda) + N(\Sigma^0)}{N_{inelastic}}$$

$$R_{\Lambda/K_s^0} = \frac{N(\Lambda) + N(\Sigma^0)}{N(K_s^0)}.$$

The main contribution to our data errors comes from the background extraction procedure.

These ratios are directly connected with multiparticle effects in complex nuclei. They also may be indicative of cascading mechanisms which may lead to enhanced Λ -production relative to non-cascading K_s^0 .

The observed Λ/K_s^0 production ratios for antideuteron-nuclei collisions and the same ratios for the events with antiproton-spectator are shown in Table IIa. They are close to those ones obtained in $\bar{p}A$ experiments at lower energies. But there is a significant difference between the peripheral and central events.

The yields of K_s^0 and Λ are presented in Table IIb; they depend on target mass, but $R(K_s^0)$ yield depends more moderately on A .

Table IIa. Production ratios R_{Λ/K_s^0} and $R_{\bar{\Lambda}/\Lambda}$ in \bar{d} -nuclei interactions at 12.2 GeV/c. Background is extracted

	$\bar{d}-d$	$\bar{d}-C'$	$\bar{d}-Pb$
R_{Λ/K_s^0} all events	0.89 ± 0.17	1.11 ± 0.32	1.98 ± 0.33
$R_{\Lambda/K_s^0} + \bar{p}$ -spectator	0.59 ± 0.23	0.63 ± 0.28	0.93 ± 0.40
$R_{\bar{\Lambda}/\Lambda}$ all events	0.68 ± 0.13	0.26 ± 0.09	0.03 ± 0.01

Table IIb. Relative yields of Λ (R_Λ), K_s^0 ($R_{K_s^0}$) and $\bar{\Lambda}$ ($R_{\bar{\Lambda}}$) (per registered primary interaction in the target). Background is extracted

	d	C'	Pb
$R_{K_s^0}$ %	2.57 ± 0.43	4.02 ± 1.16	14.5 ± 4.0
$R_{K_s^0}$ % \bar{p} -spectator events	2.37 ± 0.50	4.20 ± 1.37	11.4 ± 3.2
R_Λ %	2.24 ± 0.33	4.25 ± 1.03	27.9 ± 5.0
R_Λ % \bar{p} -spectator events	1.40 ± 0.39	2.65 ± 1.09	10.3 ± 3.6
$R_{\bar{\Lambda}}$ %	1.52 ± 0.19	1.10 ± 0.30	0.85 ± 0.24

We have also observed a dramatic difference in Λ and $\bar{\Lambda}$ productions, especially for a heavy nucleus. The yield ratio $\bar{\Lambda}/\Lambda$ was found as $3 \cdot 10^{-2}$ for lead.

The behaviour of neutral strange particle production on target mass, is shown in Fig.2. It is obvious that dependencies of Λ , K_s^0 and $\bar{\Lambda}$ yields are different. At the same time, the V^0 's from peripheral interactions behave very similar. (The statistics for $\bar{\Lambda}$'s is insufficient, and the data are not shown for stripping events).

The difference in yields for peripheral and central interactions is very surprising. The mean values of antideuteron impact parameters (Fig.1) show that in stripping events the second nucleon interacts very closely to the edge of the target nucleus. One could suppose that the conditions for Λ 's production if they are produced in the secondary rescattering processes, are less favourable in peripheral interactions. At the same time, it should not greatly influence K_s^0 yields, if K_s^0 -mesons appeared from the primary $\bar{N}N$ interaction.

We have also investigated the dependence of neutral strange particle production on the number of charged particles in the interaction. In Fig.3 the relative yields $R_{K_s^0}$ and R_Λ (per registered interaction in the target) are plotted as a function of the total charged multiplicity and multiplicities of «fast» and «slow» particles.

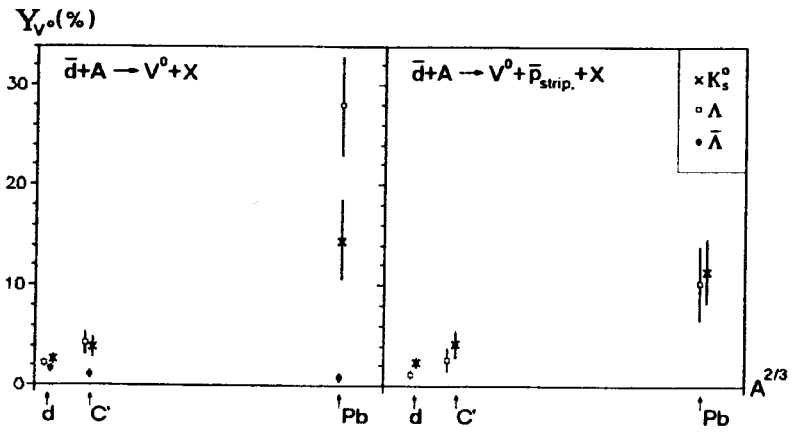


Fig.2. Relative yields of K_s^0 -, Λ - and $\bar{\Lambda}$ -particles for various nuclear targets in our experiment. Target masses are shown as $A^{2/3}$

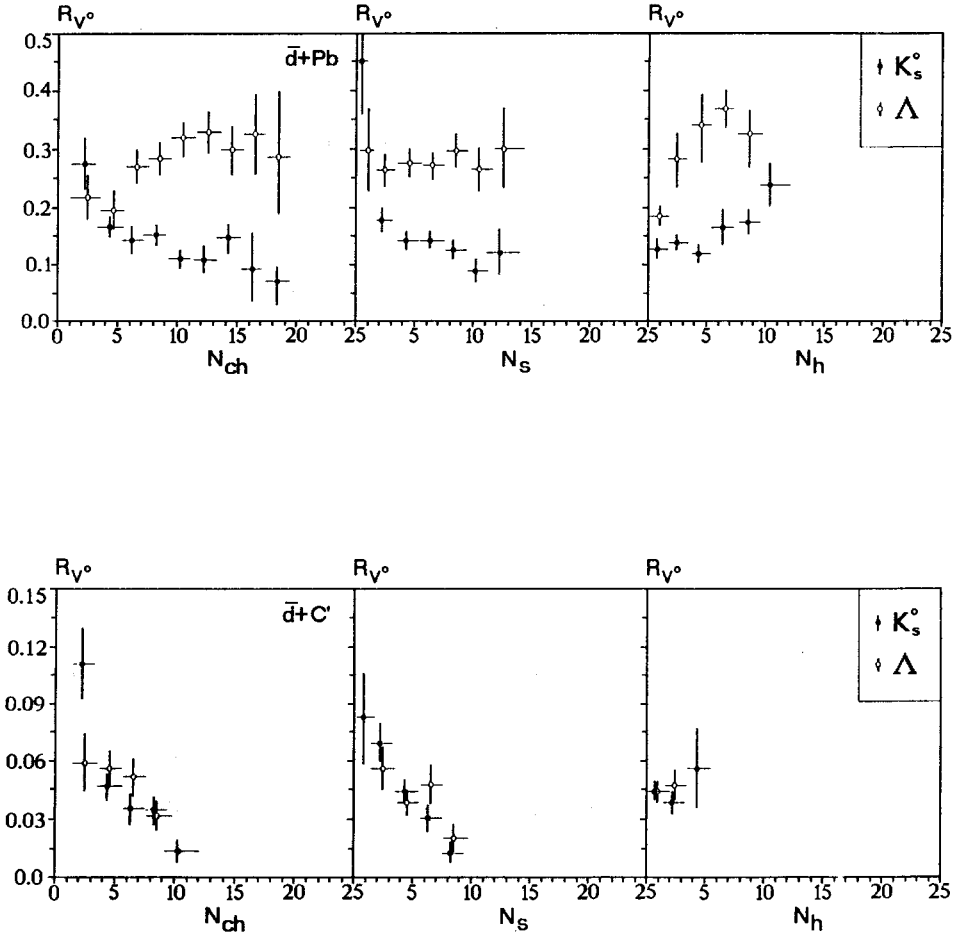


Fig.3. Yields of K_s^0 and Λ plotted as a function of n_{ch} , n_s and n_h for carbon and lead nuclei

The K_s^0 -yield is the highest in a low-multiplicity region, as the events with $n_{ch} = 1, 2, 3$ are enriched with interactions with quasi-free nucleon at the nuclear periphery. But in high-multiplicity events we observed a relative increase of Λ production (over K_s^0 production).

For carbon nucleus the data tendencies for both the strange particles are similar within the errors. At the same time, for lead nucleus the dependencies of K_s^0 and Λ yields on charged multiplicity, differ greatly. It may reflect the fact that in heavy nucleus the effects of nuclear medium become sufficient, and the production mechanisms for these particles may be different.

The number of emitted charged particles, especially slow ones, can serve a measure of the number of reinteractions inside nucleus. The dependence of Λ yield on the number of charged particles will be discussed in detail in chapter 5, in connection with the « Λ retention property» [28].

4. Rapidity Distributions

Rapidity distribution of emitted particles allows one to find the frame of reference where the distribution is centered around zero. Then the mass of the participating nuclear matter (i.e. the effective number of interacting target nucleons) be determined [2,7].

Fig.4 shows the rapidity distributions of neutral strange particles in $\bar{d}A$ interactions. The shift of rapidity distributions towards the lower values, compared to $\bar{N}N$ center of mass rapidity, was observed.

In Table III the effective targets received from the rapidity distributions measured in KEK and PS179 experiments, are given. It is shown that the effective target of 8—13 nucleons is required to produce Λ , but 1—3 nucleons are necessary for K_s^0 production. It was interpreted as if Λ 's were produced on a soft lumps consisting of several nucleons.

The masses of effective targets calculated for antideuteron interactions are also presented in Table III. They are lower than in the case of $\bar{p}A$ interactions. The data on Λ coincides with the c.m. frame of the system \bar{N} together with (5 nucleons) as an effective target. For K_s^0 the effective target is only a bit heavier than 1N in comparison with 3N at 4 GeV/c.

Table III. Number of nucleons as effective target for strangeness production in various reactions

Reaction and Momentum (GeV/c)		Effective Target (N of nucleons)	
		K_s^0	Λ
0.6	\bar{p} -Ne [10]	1	8_{-3}^{+7}
4.0	\bar{p} -Ta [7]	3	13
12.2	\bar{d} -d	1.0	2.4
12.2	\bar{d} -C'	1.2	2.8
12.2	\bar{d} -Pb	1.5	5.0

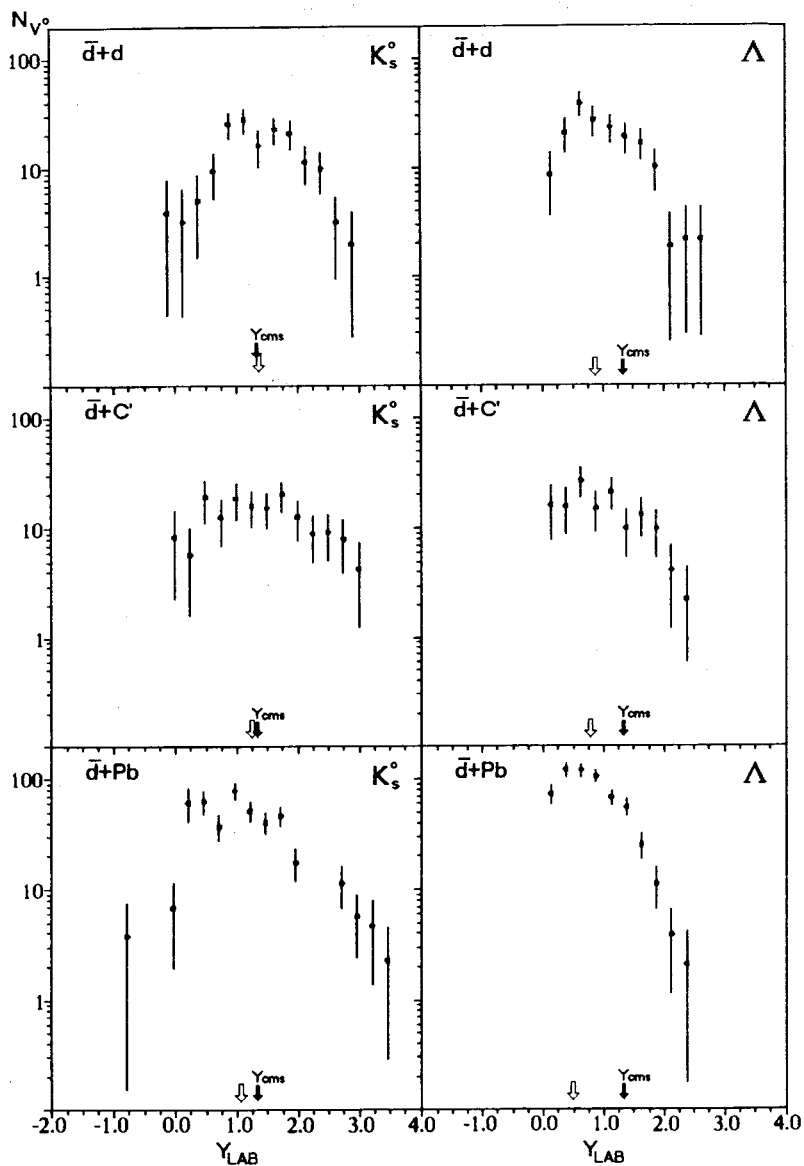


Fig.4. Rapidity distributions of neutral strange particles in $\bar{d}A$ interactions. Black arrows show the c.m.s. rapidity for NN reaction; white arrows show the centers of the W^0 's rapidity distributions

We would like to make a comment on the procedure of calculating the masses of effective targets. These calculations should strongly imply the angular symmetry of neutral strange particle emitting in a new shifted ref-

erence frame. Usually this symmetry is never observed in the experiment, as many production processes are involved, and the total angular distribution is the sum of several distributions [31], that may not necessarily have symmetrical shape.

Thus, in [7] some special cuts were done to decrease the contribution of V^0 's from the single nucleon interactions, and obtain the spherical symmetry for the spectrum of emitted particles.

In our experiment, we were not able either to obtain a symmetrical shape of angular distribution about $\cos \theta^*$ varying the effective target mass.

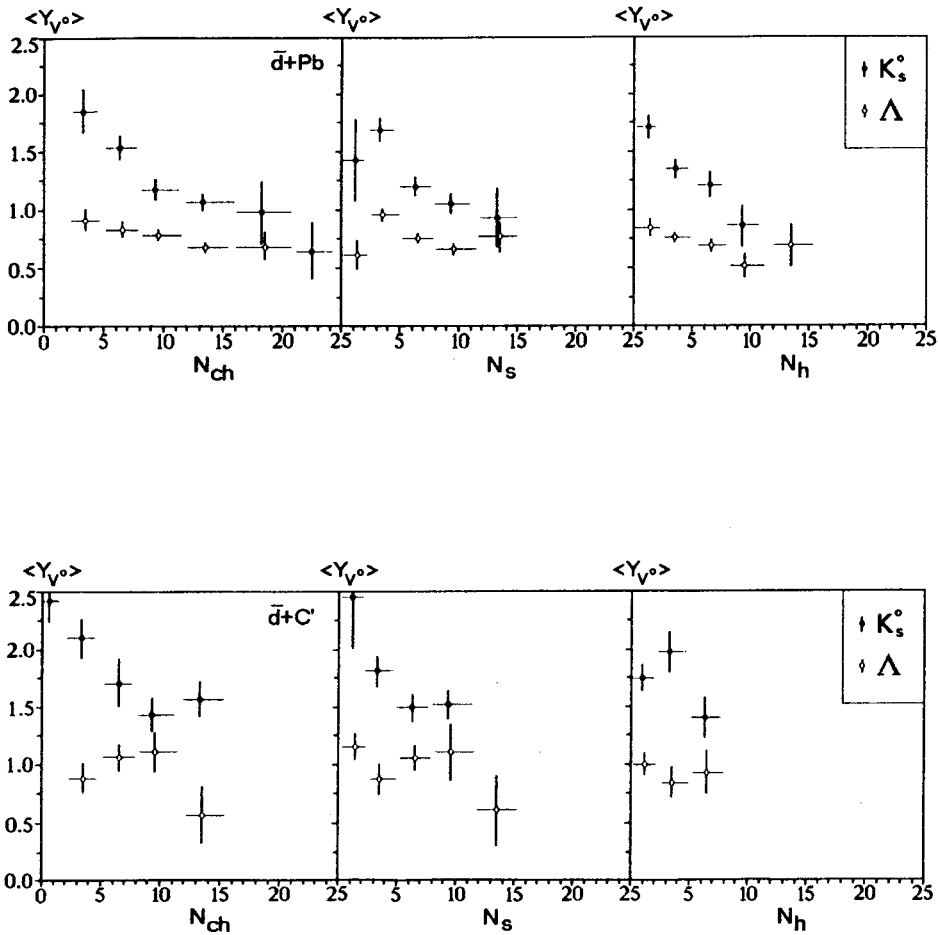


Fig.5. Mean rapidities of V^0 's plotted as functions of charged tracks multiplicity

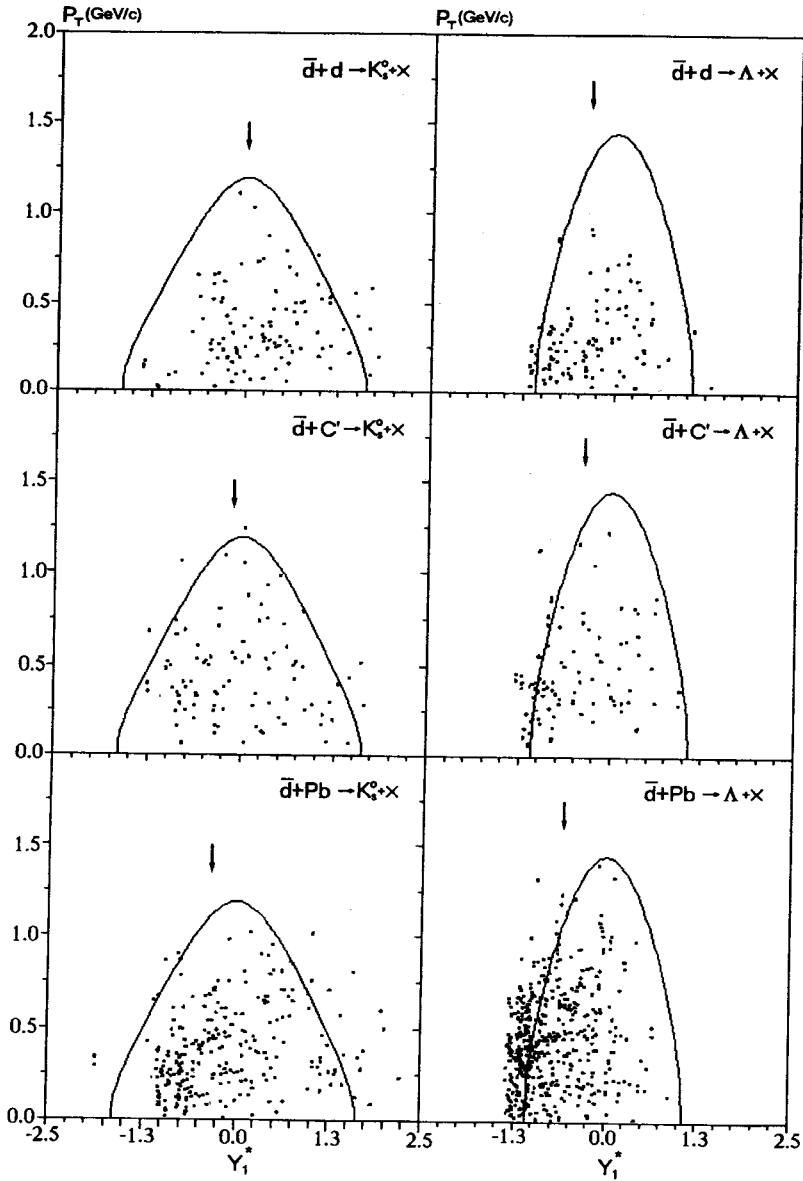


Fig.6. Scatter plots of $Y_{1-p_t}^*$. Solid curves show kinematical limits in $\bar{N}N \rightarrow K_s^0 \Lambda N$ and $\bar{N}N \rightarrow \Lambda \bar{\Lambda}$ reactions. Arrows mark the centers of rapidity distributions

Figure 5 shows the V^0 's mean rapidity $\langle Y_{lab} \rangle$ as a function of the number of charged tracks. For low multiplicities, the rapidity values are syste-

matically higher due to their shift to one-nucleon kinematics in elementary \overline{NN} processes. We could have obtained the higher values for the effective target masses and uniform angular distributions, considering only high-multiplicity events, though this procedure seems to be rather incorrect and suitable only for illustrative purpose.

Also, it is known from \overline{pp} -interactions that Λ and $\overline{\Lambda}$ behave as the fragments of the target proton and projectile antinucleon, respectively; and the rapidity distribution for Λ is always shifted towards lower rapidity relatively to \overline{NN} center-of-mass reference frame. Using these calculations for \overline{pp} interaction at 4 GeV/c, we could have obtained the mass of the effective target equal to 5—6 nucleons, (Fig. 10 in Ref. [7]), but that is of no physical sense.

In our experiment the calculated mass of effective target for Λ is about (5 nucleons) in the lead nucleus. But if one calculates the rapidity shift not from \overline{NN} -c.m.s., but from the system obtained using mean rapidity values for Λ in \overline{pp} or \overline{dd} -interactions, the effective target mass would become lower than the three-nucleon mass.

To show the difference from \overline{NN} -kinematics, scatter plots $Y_{1-p_t}^*$ for K_s^0 and Λ in \overline{dA} -interactions are presented in Fig. 6. (Y_1^* is the V^0 's rapidity in \overline{NN} c.m.s.). The solid curves indicate the kinematical limits for V^0 's in elementary processes $\overline{NN} \rightarrow K_s^0 \Lambda N$ and $\overline{NN} \rightarrow \Lambda \overline{\Lambda}$. The data points for K_s^0 lie uniformly inside the kinematical boundaries, but the points for Λ 's are shifted towards the lower boundary, and for \overline{d} -Pb interactions about 35% of Λ 's lie outside this region. It may indicate that some collective multinucleon processes were involved in the Λ 's production on a heavy nucleus, contrary to the K_s^0 production.

5. Mean Multiplicities of Associated Charged Particles

The average charged prong multiplicities at the production vertices with and without associated V^0 's are presented in Table IV. The mean multiplicities $\langle n_s \rangle$ and $\langle n_h \rangle$ are also given. The «h»- and «s»-particles are the particles with the velocities $\beta > 0.7$ and $\beta < 0.7$, respectively. The separation point $\beta = 0.7$ between fast (= «shower») and slow (= «heavy») tracks is the same as in the emulsion experiments.

The real multiplicities in $\bar{d}A$ interactions are higher than those in Table IV, because in our experiment most of the charged particles with the momenta lower than 100–200 MeV/c are surely to be absorbed in the targets.

In the lower part of Table IV the data for \bar{d} -Pb interactions with observed \bar{p} -spectator are also presented. These values are obviously much smaller than ones for all \bar{d} -Pb interactions. This fact proves our conclusion about the peripheral character of these interactions.

Table IV. Corrected mean charged multiplicities for \bar{d} -nuclei collisions. Charged multiplicities from events with antiproton-spectator are marked by asterisk. Background is extracted

LEXAN			
	Without V^0	With K_S^0	With Λ
n_{ch}	9.81 ± 0.23	7.00 ± 0.31	7.98 ± 0.31
n_-	4.51 ± 0.11	3.03 ± 0.16	3.28 ± 0.18
n_+	5.30 ± 0.13	3.97 ± 0.18	4.70 ± 0.22
n_s	8.36 ± 0.19	5.15 ± 0.21	5.82 ± 0.34
n_h	1.45 ± 0.11	1.85 ± 0.20	2.16 ± 0.11
LEAD			
	Without V^0	With K_S^0	With Λ
n_{ch}	14.52 ± 0.15	14.37 ± 0.31	14.59 ± 0.31
	$7.54 \pm 0.58^*$		$6.67 \pm 1.04^*$
n_-	4.12 ± 0.09	3.23 ± 0.10	2.76 ± 0.09
	$2.71 \pm 0.24^*$		$2.21 \pm 1.41^*$
n_+	10.40 ± 0.22	11.14 ± 0.27	11.83 ± 0.19
	$4.82 \pm 0.42^*$		$4.46 \pm 0.71^*$
n_s	8.62 ± 0.19	7.86 ± 0.20	7.12 ± 0.17
	$4.71 \pm 0.57^*$		$4.35 \pm 0.60^*$
n_h	5.90 ± 0.17	6.51 ± 0.21	7.48 ± 0.15
	$2.83 \pm 0.60^*$		$2.32 \pm 0.50^*$

The main features of multiplicity characteristics are seen as follows:

- n_s and n_- depend weakly on target mass;
- for the events with neutral strange particles n_s is smaller than for the ordinary events;
- for the events with Λ particle $\langle n_h \rangle$ always exceeds $\langle n_h \rangle$ value for the events without Λ production. It may indicate the importance of secondary reinteraction processes for strangeness production.

Nikolaev [28] puts out the concept of « Λ retention property»: once Λ was produced in fragmentation of a target nucleon, it was not absorbed, but the K^0/\bar{K}^0 could reinteract, disappear and produce Λ .

Λ 's production is very sensitive to any reabsorption of the produced particles, followed by the generation of surplus Λ 's. The number of h -particles was traditionally considered as a measure of the number of projectile collisions and secondary reinteractions inside the nucleus [28—30]. The resulting increase of mean multiplicity of the charged and h -particles in the events containing Λ was also predicted.

The observed dependence of Λ 's production yield on n_{ch} and n_h for \bar{d} -Pb collisions (Fig.3) is in agreement with the prediction of [28].

6. Kinematical Characteristics of Neutral Strange Particle

In Table Va some kinematical characteristics of neutral strange particles are given.

The difference between the Λ and K_s^0 and mean momenta for all the target masses reflects the difference in production mechanisms for these particles. Also, for the lead nucleus, the mean values for the neutral strange particles momentum are lower than the values for light nuclei.

The influence of number medium turns out to be sufficient for both: the K_s^0 and the Λ spectra. For the deuterium target, one can assume that K_s^0 -mesons are produced mostly in elementary $\bar{N}N$ interactions; but for a heavy nucleus this assumption seems to be simplified. The cross section of strangeness-exchange reactions like $\bar{K}N \rightarrow \Lambda \pi$ is a decreasing function of a kaon momentum [24], so one could expect that the spectrum of emitted K_s^0 should be enriched with the high-momentum component. The data of our experiment do not prove this suggestion.

Table Va. Kinematical characteristics of neutral strange particle in \bar{d} -A interactions.
All values are given in (GeV/c), (GeV/c)²

	\bar{d} -d	\bar{d} -C'	\bar{d} -Pb
$\langle p_t \rangle K_s^0$	0.349 ± 0.023	0.430 ± 0.027	0.431 ± 0.016
$\langle p_t^2 \rangle K_s^0$	0.172 ± 0.023	0.236 ± 0.028	0.222 ± 0.016
$\langle P \rangle K_s^0$	2.14 ± 0.25	2.03 ± 0.25	1.28 ± 0.17
$\langle p_t \rangle \Lambda$	0.295 ± 0.021	0.487 ± 0.034	0.457 ± 0.015
$\langle p_t^2 \rangle \Lambda$	0.124 ± 0.017	0.297 ± 0.041	0.279 ± 0.017
$\langle P \rangle \Lambda$	1.52 ± 0.20	1.60 ± 0.21	1.16 ± 0.09

Table Vb. The inverse slope paramteres (MeV)
for neutral strange particles momentum spectra at various energies

Reaction Momentum (GeV/c)	\bar{d} -d 12.2	\bar{d} -C' 12.2	\bar{d} -Pb 12.2	\bar{d} -Ta [7] 4	\bar{d} -Xe [12] at rest	\bar{d} -Xe [16] 200
T^0 from $P^* K_s^0$	110 ± 10	169 ± 14	172 ± 11	135 ± 13	117 ± 15	173 ± 22
T^0 from $p_t K_s^0$	104 ± 14	145 ± 17	158 ± 12			
T^0 from $P^* \Lambda$	88 ± 9	119 ± 28	138 ± 11	97 ± 6	53 ± 9	144 ± 17
T^0 from $p_t \Lambda$	81 ± 19	108 ± 20	119 ± 9			

The neutral strange particles momentum spectra were fitted to relativistic Maxwell-Boltzmann distribution $dN/dp = A(p^2/E) \exp(-E/T^0)$ [12,14], where the normalization constant A and the temperature T^0 are experimental parameters. For comparison with the other experiments, the fit was fulfilled in the reference system where $\langle Y^* \rangle$ is equal to zero. All the spectra were described satisfactory using one temperature parameter.

Figure 7 presents the distributions of the transverse momentum squared for K_s^0 and Λ particles. These distributions were fitted to an exponential form $A \exp(-Bm_t)$, where m_t is the transverse mass.

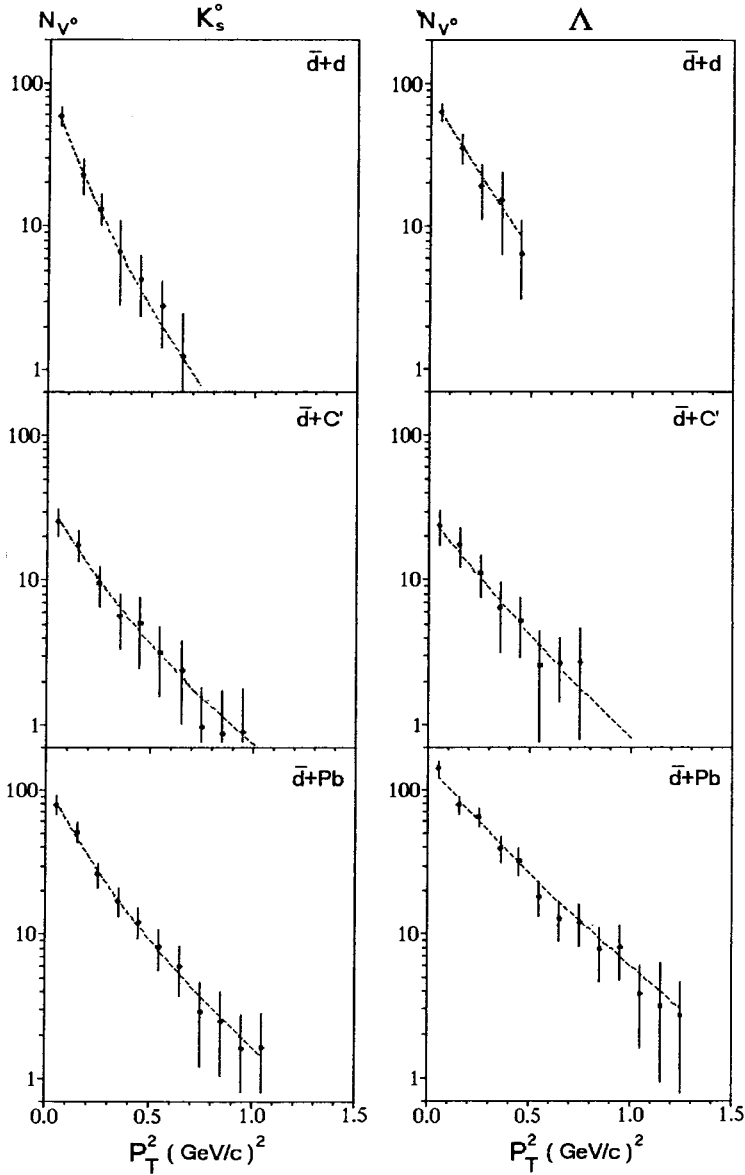


Fig. 7. P_T^2 distributions of V^0 -particles in $\bar{d}A$ -interactions. The fit is explained in the text

The values for inverse slope parameters T^0 and $1/B$ in both: the momentum and the transverse momentum fits, are given in Table Vb. They are close to those obtained in $\bar{p}A$ -interactions [7, 12, 16].

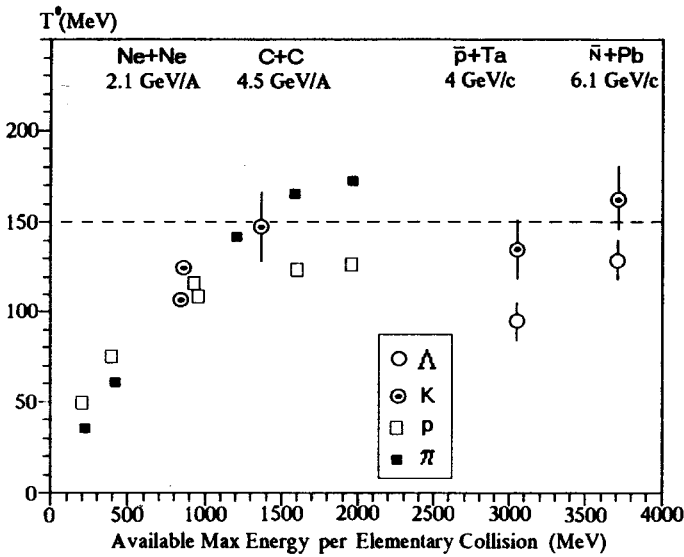


Fig.8. The slope parameters versus «available maximum energy per elementary collision» in various nuclear reactions (Ref. [32])

Figure 8 shows a summary of the parameter T^0 plotted versus «available maximum energy per elementary collision», which is defined as

$$E = \sqrt{s} - 2M_p \text{ for proton-induced}$$

and $E = \sqrt{s}$ for antiproton-induced reactions.

The picture is taken from [32]. The parameter T^0 for \bar{d} -Pb interactions does not differ greatly from the values obtained in \bar{p} -nucleus or ion collisions.

The dashed line indicates the lowest estimate of the critical temperature for qg -plasma transition; though the more realistic estimation for $T_{critical}^0$ is about 220 MeV at corresponding energy density $1-2 \text{ GeV}/\text{fm}^3$ [33].

In Table VI the kinematical characteristics on negative hadrons in $\bar{d}A$ interactions are presented. These characteristics seem to be not very sensitive to the reaction mechanism, contrary to neutral strange particles.

In Fig.9 we compare the rapidity distributions of negative tracks (mostly pions) produced in interactions with Λ -particles and in ordinary interactions. The observed shift towards the lower rapidity may indicate the presence of a more developed cascade in Λ -containing events; though it could

Table VI. Kinematical characteristics of negative charged particles in $\bar{d}A$ interactions. T^0 is deduced from p_t^2 -distributions

$\bar{d}-C'$			
	Without V^0	With K_S^0	With Λ
$\langle p_t \rangle$ (GeV/c)	0.233 ± 0.008	0.300 ± 0.018	0.276 ± 0.017
$\langle p_t^2 \rangle$ (GeV/c) ²	0.102 ± 0.007	0.147 ± 0.016	0.124 ± 0.015
T^0 (MeV)	102 ± 5	136 ± 13	113 ± 9
$\langle P \rangle$ (GeV/c)	0.962 ± 0.038	1.127 ± 0.089	1.053 ± 0.101
$\langle Y \rangle$	1.522 ± 0.034	1.435 ± 0.068	1.421 ± 0.066
$\bar{d}-Pb$			
	Without V^0	With K_S^0	With Λ
$\langle p_t \rangle$ (GeV/c)	0.264 ± 0.007	0.258 ± 0.009	0.268 ± 0.008
$\langle p_t^2 \rangle$ (GeV/c) ²	0.112 ± 0.006	0.108 ± 0.008	0.125 ± 0.011
T^0 (MeV)	116 ± 4	103 ± 5	108 ± 5
$\langle P \rangle$ (GeV/c)	0.811 ± 0.030	0.688 ± 0.033	0.646 ± 0.027
$\langle Y \rangle$	1.240 ± 0.028	1.046 ± 0.037	0.952 ± 0.029

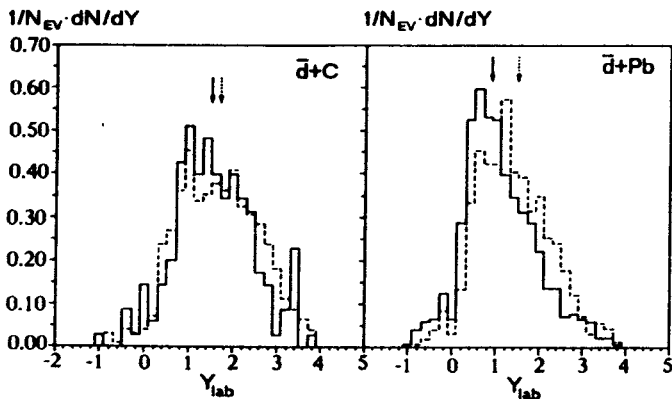


Fig.9. Normalized lab rapidity distributions of negative hadrons for Λ -events (solid line) and ordinary events (dashed line) in $\bar{d}-C'$ and $\bar{d}-Pb$ collisions

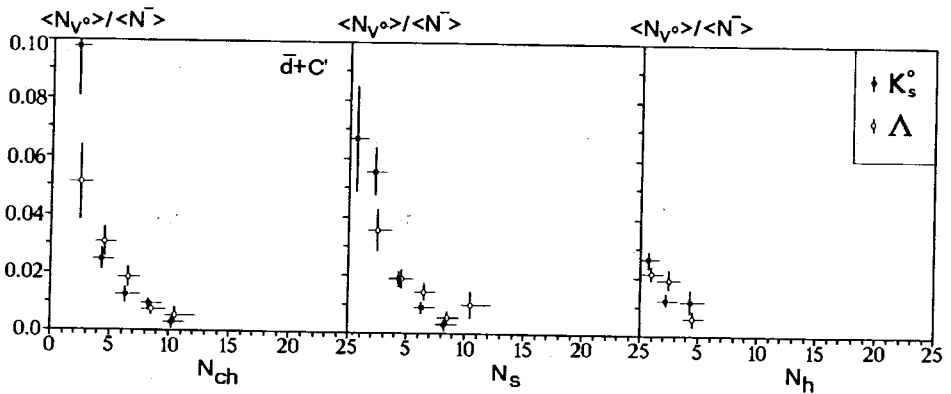
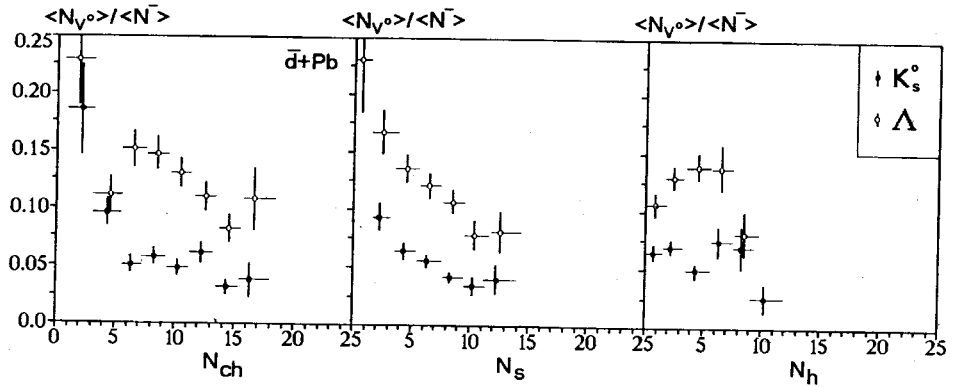


Fig. 10. The dependence of the production ratios Λ/h^- and K_s^0/h^- on the charged tracks multiplicity

be explained that less energy is available for π 's production in these events due to the limited phase space.

In Fig. 10 the dependencies of the production ratios Λ/h^- and K_s^0/h^- (strange/to non-strange) as the function of the associated charged tracks multiplicity are shown. The behavior of these ratios also indicates clearly that different production processes are important in Λ and K_s^0 cases and for heavy/light nuclei.

7. Conclusion

We have studied the neutral strange particle production in antideuteron-nuclei interactions at 12.2 GeV/c. Our results are in agreement with the data from the antiproton experiments at various energies and nuclear targets. The main results can be summarized as follows:

- In \bar{d} -nuclei interactions, the Λ production cross section is enhanced. The yield of Λ is almost equal to yield of K_s^0 even for a deuterium nucleus, but equal to 2 in \bar{d} Pb interactions. For lead, the Λ production cross section is a substantial part of the total inelastic cross section.

- The dramatic difference in Λ and $\bar{\Lambda}$ productions in $\bar{d}A$ interaction was observed. The ratio $R_{\bar{\Lambda}/\Lambda}$ turned out be small: 3×10^{-2} for the lead target.

- The yield of Λ particles in peripheral interactions is suppressed if to be compared with yields in non-peripheral case. At the same time, the «periphericity» of the interaction does not influence significantly the K_s^0 yields.

- The dependence of production yields on target mass is different for Λ^- , K_s^0 and $\bar{\Lambda}$ -particles. At the same time, the data on V^0 from peripheral interactions show the similar trend.

- The observed difference in relative yields of Λ -particles in antideuteron-deuteron interactions with and without stripping antiproton, may reflect the sufficient role of rescattering processes for Λ production even in the simplest deuteron nucleus in spite of its poor structure.

- Rapidity distributions for Λ 's show strong deviation from one-nucleon kinematics. It may indicate the important role of collective multinucleon processes in Λ production on heavy nucleus, contrary to K_s^0 production.

- The enhancement of grey track multiplicity is observed in the events with Λ -hyperons. This fact could be interpreted as a signal of a more developed cascade in nucleus. The relative increase of Λ -production while n_{ch} and n_h growing is in accordance with the prediction of [28].

- The difference in kinematical characteristics of Λ and K_s^0 is observed. It may reflect the importance of different production mechanisms for Λ and K_s^0 particles. Our data allows one to suggest that Λ particles are produced in secondary reinteractions and rescattering processes.

The authors are grateful to S.Yu.Schmakov and V.V.Uzhinskii. Their help in background simulation and calculations using DIAGEN code, was very important for our studies.

References

1. Kerbikov B.O. et al. — Uspekhi Fiz. Nauk, 1989, 159, p.1.
2. Cuaraldo C. — Nuovo Cim., 1989, 102A, p.1137.
3. Rafelski J. — Phys. Lett., 1980, 91B, p.281.
4. Koch P., Muller B., Rafelski J. — Phys. Rep., 1986, 142, p.168.
5. Koch P. — Prepr. of Regensburg Univ., TPR-90-58, 1990.
6. Condo G.T. et al. — Phys. Rev., 1984, C29, p.1531.
7. Miyano K. et al. — Phys. Rev., 1988, C38, p.2788.
8. Batusov Yu.A. et al. — JINR E1-90-118, Dubna, 1990.
9. Batusov Yu.A. et al. — Yad. Fiz., 1989, 50, 1524.
10. Balestra F. et al. — Phys. Lett., 1987, B194, p.192.
11. Balestra F. et al. — Nucl. Phys., 1991, A526, p.415.
12. Andryakov A.D. et al. — Prepr. ITEP 104-90, Moscow, 1990.
13. Dolgonenko A. — Yad. Fiz., 1992, 55, p.1253.
14. Reidlberger J. et al. — Phys. Rev., 1989, C40, p.2717.
15. Batyunia B.V. et al. — JINR E1-93-20, Dubna, 1993.
16. Derado I. et al. — Z. Phys. C — Particles and Fields, 1991, 50, p.31.
17. Rafelski J. — Phys. Lett., 1988, B207, p.371.
18. Cugnon J., Vandermeulen J. — Phys. Lett., 1984, 146B, p.16.
19. Cugnon J., Vandermeulen J. — Phys. Rev., 1989, C39, p.181.
20. Dover C.B., Koch P. — Prepr. BNL-42105, 1988.
21. Kharzeev D.E., Sapozhnikov M.G. — JINR E4-88-930, Dubna, 1988.
22. Kharzeev D.E., Sapozhnikov M.G. — JINR E4-91-104, Dubna, 1991.
23. Gibbs W.R., Kruk J.W. — Phys. Lett., 1990, B237, p.317.
24. Cugnon J., Deneye P., Vandermeulen J. — Phys. Rev., 1990, C41, p.1701.
25. Strottman D., Gibbs W.R. — Phys. Lett., 1984, 149B, p.288.
26. Cugnon J. — Nucl. Phys., 1992, A542, p.559.
27. Schmakov S.Yu. et al. — Comp. Phys. Comm., 1989, 54, p.125.
28. Nikolaev N.N. — Z. Phys. C — Particles and Fields, 1989, 44, p.645.
29. De Marzo C. et al. — Phys. Rev., 1984, D29, p.2476.
30. Faessler M.A. et al. — Nucl. Phys., 1979, B157, p.1.
31. Balestra F. et al. — Phys. Lett., 1989, B217, p.43.
32. Nakai K. — Nucl. Phys., 1988, A479, p.311.
33. McLerran L. — In: The Elementary Structure of Matter, ed. J.-M. Richard, Springer-Verlag, Berlin, 1988, p.320.
34. Mohring H.-J., Ranft J. — Z. Phys. C — Particles and Fields, 1991, 52, p.643.
35. Formanek J. — Prepr. Orsay IPNO/TH 81-10, 1981.

Received on February 15, 1993.